Modal-S-Matrix Design of Optimum Stepped Ridged and Finned Waveguide Transformers

JENS BORNEMANN AND FRITZ ARNDT, SENIOR MEMBER, IEEE

Abstract —Optimum stepped transformers from rectangular waveguide to ridged and all-metal finned waveguides are designed with the method of field expansion into eigenmodes, which includes higher order mode interaction between the step discontinuities. Computer-optimized design data are given for a Ku-band ridged waveguide prototype with a ridge width of 1 mm, as well as for Ka-band and E-band finned waveguide transformers with commercially available metal fin thicknesses of 0.19 mm and 0.1 mm, respectively, suitable for metal-etching manufacturing technique. The optimum designs achieve a minimum return loss of about 36 dB, or 34 dB for the whole Ka- or E-band, respectively. The theory is verified by comparison with measured results.

I. INTRODUCTION

RIDGED WAVEGUIDES [1]–[6] and their important variant with thin ridges (which is usually designed as a "planar circuit" [7]–[9], "finned waveguide" [5], or "all-metal finline" [10]) have found many applications in microwave and millimeter-wave devices [1]–[12]. The advantages of these circuits include large bandwidths, low characteristic impedances, and, in its finned version, the possibility of low-cost, low-loss E-plane integrated circuit designs [8]–[12]. Of particular importance are the transition between ridged or finned waveguides of different gap height and the transition to the rectangular waveguide. This paper introduces an exact field theory design of optimum stepped ridged and finned waveguide transformers (Fig. 1).

While many papers have appeared recently on the problem of finline discontinuities [13]–[21], among three-dimensional ridged waveguide or all-metal finline structures only short end effects [9] and gradual tapers [10] have been investigated so far with analytical methods. Moreover, with the exception of the variational method in [9] for calculating short end effects and the generalized telegraphist's equation method in [19] for calculating gradual unilateral finline tapers, most of the techniques presented for the analysis of finline or all-metal finline discontinuities (the equivalent circuit methods in [13]–[18] and [20], the variational method in [21], and the spectral-domain method in [10]) neglect the influence of the finite metallization thickness, which has turned out to be important for all-metal finline constructions (cf. [22]–[24]).
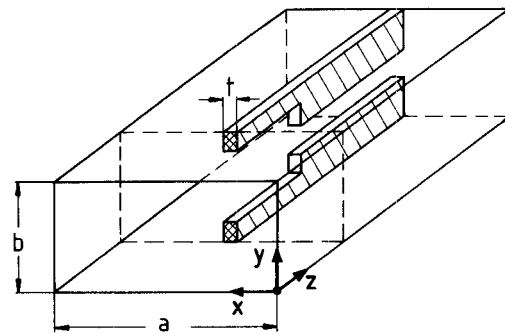
Fig. 1. Ridged or finned waveguide step transformer structure.

Although there are no hybrid modes [28]–[30] on ridged and finned waveguides to be considered, the three-dimensional discontinuities of the form of Fig. 1, like double-plane steps in waveguides [27], require all field components as well as the TE- to TM-mode coupling to be taken into account. The theory given in this paper, which includes higher order mode coupling effects as well as the finite ridge or metal fin width, is based on modal field expansion into orthogonal eigenmodes [22]–[31]. An optimization procedure based on a modified direct search method where the parameters of the error function are varied statistically [32] leads to optimum stepped transformer designs. Comparison with linearly tapered transformer sections of equal length (approximated by a stepped function) shows the advantage provided by the optimum stepped design. The design data given may be transferred into other waveguide bands by suitable frequency scaling relations which include the metal fin thickness. Measured results verify the theory.

II. THEORY

For the computer-aided design of ridged and finned waveguide transformers, the modal-S-matrix method [22]–[24], [27], [35] is applied, which has already proved to be highly appropriate for the accurate design of millimeter-wave components. Similar to the field theory treatment of E-plane filters or couplers (cf. [22]–[24], [35]), the transformer structure (Fig. 1) is decomposed into appropriate key building blocks (homogeneous rectangular waveguide, step discontinuity waveguide to finned waveguide, homogeneous finned waveguide, Fig. 2), and the

overall scattering matrix of the total transformer is calculated by suitable direct combination of all single modal scattering matrices. Therefore, the more general part of the theory is given here in abbreviated form only; for details, the reader is referred to [22]–[24], [27], and [35]. The derivation of the required key building block S-matrix for the step discontinuity waveguide to finned waveguide, however, is new and quite different from the one already given in, e.g., [22] or [35], since another class of modal fields is involved. Note that for the inverse structure (discontinuity finned waveguide to waveguide), the related scattering matrix is simply derived by merely interchanging the corresponding submatrix elements.

H-plane or E-plane discontinuities (as in [22] or [35]) require only TE_{m0} or TE_{mn}^x modes, respectively, to be considered. For the rigorous field theory treatment of the three-dimensional step discontinuity problem shown in Fig. 2, however, a superposition of all TE_{mn} as well as TM_{mn} modes is necessary, and the TE- to TM-mode coupling effect [27] has to be taken into account. This is due to x-, y-, and z-dependent field distortions at $z = 0$, l (Fig. 2). The electromagnetic field [25], [26] in the subregions $i =$ I, II (Fig. 2):

$$\vec{E}^i = \nabla \times \left(A^i_{Hz} \vec{e}_z \right) + \frac{1}{j\omega\epsilon} \nabla \times \nabla \times \left(A^i_{Ez} \vec{e}_z \right)$$

$$\vec{H}^i = \nabla \times \left(A^i_{Ez} \vec{e}_z \right) - \frac{1}{j\omega\mu} \nabla \times \nabla \times \left(A^i_{Hz} \vec{e}_z \right) \qquad (1)$$

is therefore derived from the z-components of two vector potentials:

$$\vec{A}^i_{Hz} = \sum_{q=1}^{\infty} \left(\sqrt{Z^i_{Hq}} \right) \cdot T^i_{Hq}(x, y)$$

$$\cdot \left[V^i_{Hq} \exp\left(- jk^i_{zHq} z \right) + R^i_{Hq} \exp\left(+ jk^i_{zHq} z \right) \right] \quad (2)$$

$$\vec{A}^i_{Ez} = \sum_{p=1}^{\infty} \left(\sqrt{Y^i_{Ep}} \right) \cdot T^i_{Ep}(x, y)$$

$$\cdot \left[V^i_{Ep} \exp\left(- jk^i_{zEp} z \right) - R^i_{Ep} \exp\left(+ jk^i_{zEp} z \right) \right]$$

with the wave impedances [25]

$$Z^i_{Hq} = (\omega\mu_0) / \left(k^i_{zHq} \right) = 1 / Y^i_{Hq}$$

$$Y^i_{Ep} = (\omega\epsilon_0) / \left(k^i_{zEp} \right) = 1 / Z^i_{Ep}. \qquad (3)$$

$V^i_{H,E}$, $R^i_{H,E}$ are the still unknown TE-, TM-mode wave amplitudes of the forward and backward waves, respectively; k_z is the propagation factor; and T^i_{Hq}, T^i_{Ep} are the cross-section eigenfunctions according to the given waveguide boundaries.

The functions T^i_{Hq} and T^i_{Ep} in (2) may conveniently be simplified utilizing the magnetic wall (m.w.) and electric wall (e.w.) symmetries at $x = a/2$, and $y = b/2$, respectively (cf. Fig. 2(a) and (b)). For region II, the eigenvalue problem may be formulated advantageously using the transverse resonance method [28]–[30], where the boundary conditions to be applied in the x direction (electric wall at
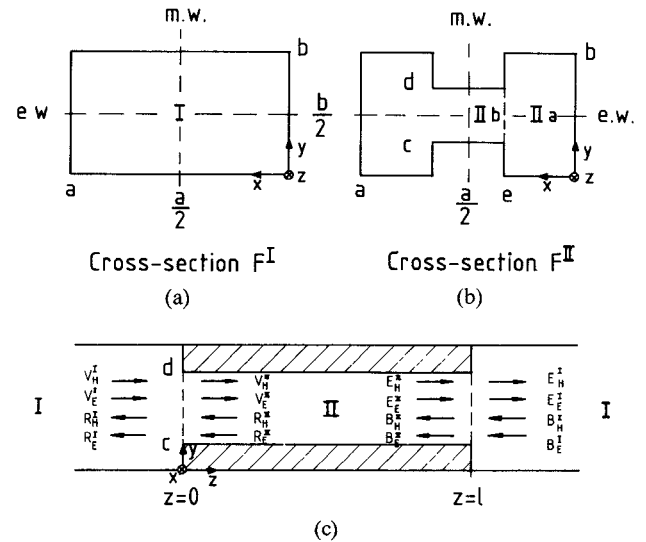

Fig. 2. Configuration for the rigorous field theory treatment. (a) Waveguide (m.w. = magnetic wall, e.w. = electric wall). (b) Ridged or finned waveguide. (c) Forward and backward waves at the step discontinuities at $z = 0$ and $z = l$, respectively.

$x = 0$, magnetic wall at $x = a/2$, cf. Fig. 2(b)) provide the corresponding homogeneous system of equations. The cross-section eigenfunctions of the rectangular waveguide section I (Fig. 2(a)) and of the ridged or finned waveguide structure II (Fig. 2b), are given in the Appendix.

In order to obtain the modal scattering matrix directly by the field matching relations of the wave amplitude coefficients according to (2), the cross-section eigenfunctions are suitably normalized [25], [27] so that for a wave amplitude of $1\sqrt{W}$ the total power carried by the corresponding eigenmode is

$$P^i_M = \int_{F^i} \left(\vec{E}^i_M \times \vec{H}^{i*}_M \right) \vec{e}_z \, dF = \sqrt{Z^i_M} \sqrt{Y^{i*}_M} \int_{F^i} \left[\text{grad } T^i_M \right]^2 dF$$

$$= \begin{bmatrix} 1W \\ jW \\ -jW \end{bmatrix} \begin{array}{l} \text{for propagating modes} \\ \text{for evanescent TE modes} \\ \text{for evanescent TM modes.} \end{array} \qquad (4)$$

In (4), the subscript M replaces the indices Hq and Ep (cf. (2), (3)) for TE and TM modes, respectively. In region II, the relations between the amplitude coefficients in subregions IIa and IIb are given by the transverse resonance condition [28]–[30].

Matching the tangential field components of regions I and II at the common interface at $z = 0$ (Fig. 2(c)), as in [22]–[24], [27], [35], yields the modal scattering matrix (S_S) of the step discontinuity waveguide to ridged or finned waveguide:

$$\begin{bmatrix} (R^I) \\ (V^{II}) \end{bmatrix} = (S_S) \begin{bmatrix} (V^I) \\ (R^{II}) \end{bmatrix} \qquad (5)$$

where the submatrices are given in the Appendix.

The modal scattering matrix (S_R) of the combined structure step discontinuity to ridged or finned waveguide, homogeneous ridged or finned waveguide section of finite length l, and step discontinuity back to waveguide (cf. Fig.

2(c)):

$$\begin{bmatrix} (R^{\mathrm{I}}) \\ (E^{\mathrm{I}}) \end{bmatrix} = (S_R) \begin{bmatrix} (V^{\mathrm{I}}) \\ (B^{\mathrm{I}}) \end{bmatrix} \qquad (6)$$

is calculated by suitably combining the related wave amplitude vectors. The submatrices of (6), again, are elucidated in the Appendix.

The series of steps for a complete transformer section is calculated by direct combination of the single scattering matrices (6) according to [27], the lengths of the intermediate homogeneous waveguide sections I (Fig. 2(c)) being reduced to zero for calculating the step discontinuities from one fin height to another. Contrary to the usual treatment with transmission matrices, this procedure preserves numerical accuracy, as the expressions contain exponential functions with only negative arguments. Moreover, no symmetry of the number of modes at the discontinuity is required. This fact allows one to modify adequately the number of modes [33], [34], if necessary, along the structure to be considered.

III. DESIGN

As with metal insert filters [22]–[24], the computer-aided design is carried out by an optimizing program applying the evolution strategy method [32]. An error function

$$F(\bar{x}) = \sum_{v=1}^{V} \left(|S_{11D}|^2 / |S_{11}(\bar{x}, f_v)|^2 \right) \qquad (7)$$
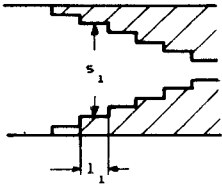
is minimized with respect to the parameter vector $(\bar{x}) = (s_1, s_2, s_3, \cdots ; l_1, l_2, l_3, \cdots)^T$. Here, f_v are the frequency sample points within the desired passband, and S_{11D} and S_{11} are the desired and calculated reflection coefficients, respectively, in decibels. The number V of frequency sample points was chosen to be equal to about 20. For given waveguide housing dimensions a and b, thickness t of the metal fins, slot width s_{fin} of the finned waveguide, and number NT of transformer sections, the parameters $\bar{x}$ to be optimized are the slotwidth s_i and the length l_i of the ith transformer section (cf. Table I).

The advantages of the applied evolution strategy method [32], i.e., a suitably modified direct search procedure, are such that no differentiation step in the optimization process is necessary; hence, the problem of local minima may be circumvented. A main optimization strategy parameter H, a secondary strategy parameter G, and a standard random variable $r \in (-1, +1)$ influence the alternation of the parameter vector $(\bar{x})$ during the optimization process with the standard deviation $\sigma = H \cdot G$ [32]. The new parameters $(\bar{x})_{\mathrm{new}}$ are calculated at each iteration step by

$$(\bar{x})_{\mathrm{new}} = (\bar{x})_{\mathrm{old}} - r \cdot (\bar{x})_{\mathrm{old}} \cdot \sigma \qquad (8)$$

where $(\bar{x})_{\mathrm{old}}$ are the preceding parameters. Initial values for H and G are chosen to be $H = 0.01$, $G = 1$. G may be utilized to modify the variation of the individual parameters. After a successful trial, H is doubled; for more than three unsuccessful trials, H is halved. If the error function is minimized three times by less than 0.2 percent, the result

TABLE I
OPTIMUM STEPPED RIDGED AND FINNED WAVEGUIDE TRANSFORMERS

KU-BAND (R140 waveguide housing: 15.799mm X 7.899mm)
Ridge thickness t = 1mm
(Fig.3)

l_1 = 5.980mm, s_1 = 6.670mm; l_2 = 6.000mm, s_2 = 5.320mm;
l_3 = 7.370mm, s_3 = 4.290mm; l_4 = 6.900mm, s_4 = 3.340mm;
l_5 = 5.620mm, s_5 = 2.440mm; l_6 = 6.020mm, s_6 = 2.000mm;
(symmetrical double section transformer)

KA-BAND (R320 waveguide housing: 7.112mm X 3.556mm)
Metal fin thickness t = 0.19mm
(Fig.4)

l_1 = 3.139mm, s_1 = 2.941mm; l_2 = 3.348mm, s_2 = 2.373mm;
l_3 = 3.521mm, s_3 = 1.936mm; l_4 = 3.118mm, s_4 = 1.545mm;
l_5 = 2.835mm, s_5 = 1.176mm; l_6 = 0.000mm, s_6 = 0.100mm
(section No.6 is the finned waveguide of slot width s_6)

E-BAND (R740 waveguide housing: 3.099mm X 1.549mm)
Metal fin thickness t = 0.1mm
(Fig. 5)

l_1 = 1.290mm, s_1 = 1.283mm; l_2 = 1.455mm, s_2 = 1.029mm;
l_3 = 1.468mm, s_3 = 0.831mm; l_4 = 1.291mm, s_4 = 0.653mm;
l_5 = 1.201mm, s_5 = 0.482mm; l_6 = 0.000mm, s_6 = 0.400mm
(section No.6 is the finned waveguide of slot width s_6)

is interpreted as a local minimum. H is then multiplied by 10^4. So the optimization process begins again for a different parameter range. Note that in order to maintain physically realistic parameters, $s_i \in (s_{\mathrm{fin}}, b)$, $l_i \in (0, \lambda/2)$, an appropriate variable transformation [32] is utilized.

The initial values for the slot widths and transformer section lengths may be chosen from an equidistant subdivision according to the given data $b, s_{\mathrm{fin}}, NT, \lambda_{g\,\mathrm{mid}}$ (where $\lambda_{g\,\mathrm{mid}}$ is the guide wavelength for the midband frequency). The CPU time for a six-step transformer design was about 45 min on a Siemens-7880 computer. More favorable approximations, e.g., fundamental mode quarter wave transformer prototype dimensions together with a suitably chosen midband frequency, for the initial values, however, may reduce the computing time considerably, e.g., by a factor of 2. A quasi-lumped element approach, as suggested in [33], [34], by increasing the number of "localized" modes while reducing the interacting modes, has no significant effect on the optimization CPU time, which is influenced mainly by the number of necessary iterations and not so much by the run time of the single calculation step.

In the optimization process, eight symmetrical TE modes together with only one TM mode provide sufficient convergence behavior, which is due to the minor influence of higher order TM modes at usual E-plane integrated circuit discontinuities. Neglecting this TM mode, however, yields frequency shifts of the return loss curve up to about 5
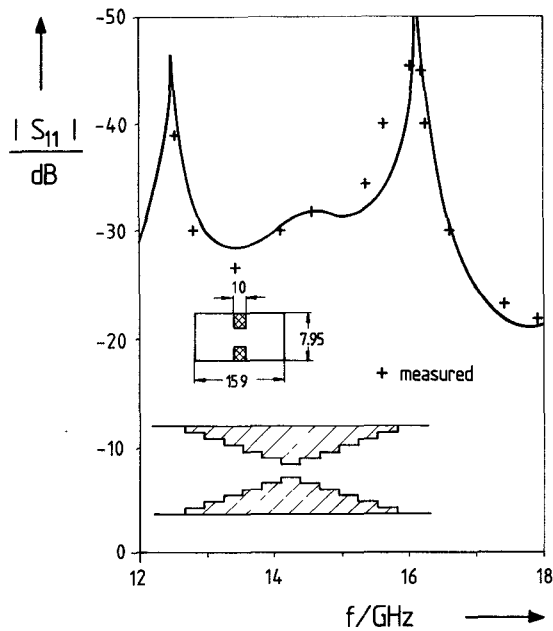
Fig. 3. Input reflection coefficient $|S_{11}|$ in decibels as a function of frequency of an optimum stepped Ku-band ridged waveguide transformer with two symmetrical five-step sections. Comparison between measurements ($++$) and theory. Waveguide dimensions in mm; for transformer dimensions, see Table I.
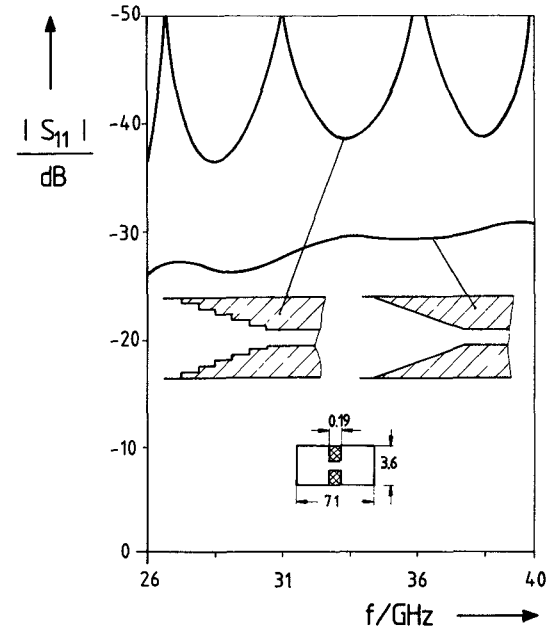

Fig. 4. Input reflection coefficient $|S_{11}|$ in decibels as a function of frequency of an optimum stepped Ka-band finned waveguide transformer with five-step sections. Comparison with a linearly tapered transformer (approximated by a 15-step function) of same length $L \approx 16$ mm. Waveguide dimensions in mm; for transformer dimensions, see Table I.

percent. The final design data are verified by considering 12 TE and seven TM modes in each transformer section.

IV. RESULTS

Fig. 3 shows the calculated and measured input reflection coefficient $|S_{11}|$ in decibels as a function of frequency of a stepped ridged waveguide transformer with two symmetrical five-step sections for the Ku-band (12–18 GHz, R140 waveguide housing: 15.799 mm×7.899 mm). The ridge width is $t=1$ mm, and the design data of the transformer are given in Table I. Good agreement between theory and measurements may be stated. The measured transmission loss was less than 0.1 dB.

As shown in Figs. 4 and 5, optimum stepped finned waveguide transformers from standard waveguide to finned waveguide of slot width of about one quarter of the corresponding waveguide height, chosen for design example, achieve minimum return losses of about 36 dB or 34 dB, for the whole Ka-band (Fig. 4) or E-band (Fig. 5), respectively. The commercially available metal fin thicknesses of 0.19 mm and 0.1 mm are highly appropriate for etched all metal finline integrated circuit designs. The comparison with linearly tapered transformer sections of the same overall length shows a significant improvement of the return loss values by the optimum stepped design, whereas the linearly tapered transformer provides better continuity of the return loss curve as a function of frequency.

The linearly tapered transformer section is simulated by means of a staircase function, stepped uniformly in height and length. Fifteen steps have turned out to yield sufficient asymptotic behavior of the input reflection coefficient.

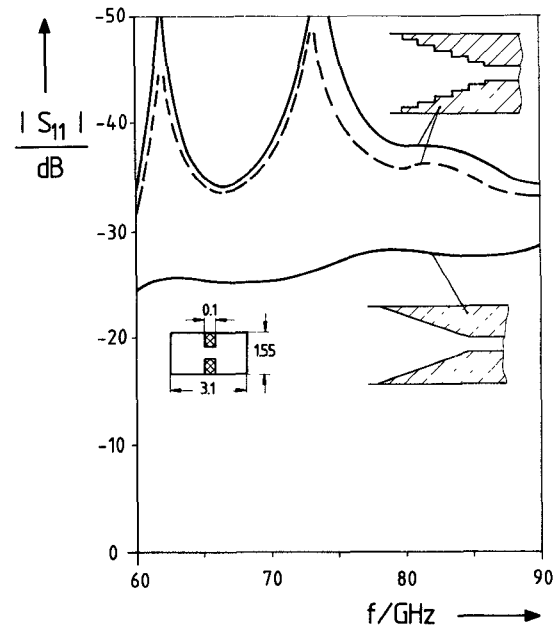The design data for the Ka-band (26–40 GHz, R320 waveguide: 7.112 mm×3.556 mm) and the E-band (60–90

Fig. 5. Input reflection coefficient $|S_{11}|$ in decibels as a function of frequency of an optimum stepped E-band finned waveguide transformer with five-step sections. Comparison with a linearly tapered transformer (approximated by a 15-step function) of same length $L \approx 6.7$ mm. Waveguide dimensions in mm; for transformer dimensions, see Table I. Tolerance analysis (dashed curve) of the optimized design for worst-case variations: strip thickness and slot widths by ± 0.01 mm, transformer section lengths by ± 0.02 mm.

GHz, R740 waveguide: 3.099 mm×1.549 mm) finned waveguide transformers are given in Table I. As has been proved by calculations using the exact method described, the design data are transferable into other common waveguide bands by suitable frequency scaling relations which should include the metal fin thicknesses.

The sensitivity of the performance of the optimized transformer to dimensional tolerances is demonstrated in Fig. 5. The dashed curve shows the input reflection coefficient for a worst-case simulation of typical sheet metal and etching tolerances (strip thickness and slot width variation ± 0.01 mm, section length variation ± 0.02 mm).

V. Conclusions

A computer-aided design of optimum stepped ridged and finned waveguide transformers is described which permits the inclusion of higher order mode coupling effects as well as the finite ridge and metal fin thickness. Application of a modified direct search method leads to optimum low input VSWR over the whole waveguide band, as has been demonstrated for Ka-band and E-band metal finline transformer design examples. The design data are transferable into other frequency bands of interest. Measurements made on a Ku-band ridge waveguide five-section transformer prototype show good agreement with theory.

with

$$\begin{bmatrix} \left(k_{xHqn}^{IIa}\right)^2 \\ \left(k_{xHqn}^{IIb}\right)^2 \end{bmatrix} = \omega^2\mu_0\epsilon_0 - \left(k_{zHq}^{II}\right)^2 - \begin{bmatrix} \left(\dfrac{2n\pi}{b}\right)^2 \\ \left(\dfrac{2n\pi}{d-c}\right)^2 \end{bmatrix}$$

$$\begin{bmatrix} \left(k_{xEpn}^{IIa}\right)^2 \\ \left(k_{xEpn}^{IIb}\right)^2 \end{bmatrix} = \omega^2\mu_0\epsilon_0 - \left(k_{zEp}^{II}\right)^2 - \begin{bmatrix} \left(\dfrac{2n\pi}{b}\right)^2 \\ \left(\dfrac{2n\pi}{d-c}\right)^2 \end{bmatrix} \quad (A3)$$

where the k_z are calculated by solving the related eigenvalue problem [28]–[30].

B. Derivation of the Modal Scattering Matrix (S_S) in (5)

Field matching at the common interface at $z = 0$ (Fig. 2c) yields

$$\sum_{q=1}^{\infty} \left(\sqrt{Z_{Hq}^I}\right)\left(\text{grad }T_{Hq}^I \times \vec{e}_z\right)\left(V_{Hq}^I + R_{Hq}^I\right) - \sum_{p=1}^{\infty} \left(\sqrt{Z_{Ep}^I}\right)\text{grad }T_{Ep}^I\left(V_{Ep}^I + R_{Ep}^I\right)$$

$$= \sum_{l=1}^{\infty} \left(\sqrt{Z_{Hl}^{II}}\right)\left(\text{grad }T_{Hl}^{II} \times \vec{e}_z\right)\left(V_{Hl}^{II} + R_{Hl}^{II}\right) - \sum_{k=1}^{\infty} \left(\sqrt{Z_{Ek}^{II}}\right)\text{grad }T_{Ek}^{II}\left(V_{Ek}^{II} + R_{Ek}^{II}\right) \quad (A4)$$

$$\sum_{q=1}^{\infty} \left(\sqrt{Y_{Hq}^I}\right)\text{grad }T_{Hq}^I\left(V_{Hq}^I - R_{Hq}^I\right) + \sum_{p=1}^{\infty} \left(\sqrt{Y_{Ep}^I}\right)\left(\text{grad }T_{Ep}^I \times \vec{e}_z\right)\left(V_{Ep}^I - R_{Ep}^I\right)$$

$$= \sum_{l=1}^{\infty} \left(\sqrt{Y_{Hl}^{II}}\right)\text{grad }T_{Hl}^{II}\left(V_{Hl}^{II} - R_{Hl}^{II}\right) + \sum_{k=1}^{\infty} \left(\sqrt{Y_{Ek}^{II}}\right)\left(\text{grad }T_{Ek}^{II} \times \vec{e}_z\right)\left(V_{Ek}^{II} - R_{Ek}^{II}\right). \quad (A5)$$

APPENDIX

A. Cross-Section Eigenfunctions T_{Hq}^i and T_{Ep}^i in (2)

Region $i = I$:

$$T_{Hq}^I(x, y) = A_q^I \cos\left[(2m-1)\frac{\pi}{a}x\right]$$

$$\cdot \left(\cos\frac{2n\pi}{b}y\right)\bigg/ \sqrt{(1+\delta_{0n})}$$

$$T_{Ep}^I(x, y) = D_p^I \sin\left[(2m-1)\frac{\pi}{a}x\right] \cdot \sin\frac{2n\pi}{b}y \quad (A1)$$

where indices q and p are related to the waveguide modes m, n by rearranging them with respect to increasing cutoff frequencies; δ_{0n} is the Kronecker delta.

Region $i = II$:

In order to eliminate the x and y dependence in the cross-section functions, (A4) is successively multiplied by $(\text{grad }T_{Hq}^I \times \vec{e}_z)$, $(-\text{grad }T_{Ep}^I)$, and (A5) by $\text{grad }T_{Hl}^{II}$, $(\text{grad }T_{Ek}^{II} \times \vec{e}_z)$.

Integration over the corresponding cross sections, using the relations [31]

$$\int_{F^i} \left(\text{grad }T_{H, Er}^i \times \vec{e}_z\right)\left(\text{grad }T_{H, Es}^i \times \vec{e}_z\right) dF$$

$$= \int_{F^i} \text{grad }T_{H, Er}^i \text{ grad }T_{H, Es}^i \, dF = \delta_{rs}$$

$$\int_{F^i} \text{grad }T_{Er}^i\left(\text{grad }T_{Hs}^i \times \vec{e}_z\right) dF$$

$$= \int_{F^i} \left(\text{grad }T_{Er}^i \times \vec{e}_z\right)\text{grad }T_{Hs}^i \, dF \equiv 0 \quad (A6)$$

$$T_{Hq}^{II}(x, y) = \sum_{n=0}^{\infty} \left[A_{qn}^{IIa} \cdot \cos\left(k_{xHqn}^{IIa}x\right) \cdot \left(\cos\frac{2n\pi}{b}y\right)\bigg/ \sqrt{(1+\delta_{0n})} \right.$$

$$\left. - A_{qn}^{IIb} \cdot \left(1/k_{xHqn}^{IIb}\right) \cdot \sin\left(k_{xHqn}^{IIb}\left(\frac{a}{2} - x\right)\right) \cdot \cos\left(\frac{2n\pi}{d-c}(y-c)\right)\bigg/ \sqrt{(1+\delta_{0n})} \right]$$

$$T_{Ep}^{II}(x, y) = \sum_{n=1}^{\infty} \left[D_{pn}^{IIa} \cdot \left(1/k_{xEpn}^{IIa}\right) \cdot \sin\left(k_{xEpn}^{IIa}x\right) \cdot \sin\left(\frac{2n\pi}{b}y\right) \right.$$

$$\left. + D_{pn}^{IIb} \cdot \cos\left(k_{xEpn}^{IIb}\left(\frac{a}{2} - x\right)\right) \cdot \sin\left(\frac{2n\pi}{d-c}(y-c)\right) \right] \quad (A2)$$

and truncation of the infinite series in (A4), (A5) provides the matrix equation system of the discontinuity at $z = 0$:

$$\text{Diag}\left\{\sqrt{Z_{Hq}^{I}}\right\}\left(V_{H}^{I} + R_{H}^{I}\right) = J_{HH}\,\text{Diag}\left\{\sqrt{Z_{Hl}^{II}}\right\}\left(V_{H}^{II} + R_{H}^{II}\right)$$

$$\text{Diag}\left\{\sqrt{Z_{Ep}^{I}}\right\}\left(V_{E}^{I} + R_{E}^{I}\right) = J_{EH}\,\text{Diag}\left\{\sqrt{Z_{Hl}^{II}}\right\}\left(V_{H}^{II} + R_{H}^{II}\right)$$

$$+ J_{EE}\,\text{Diag}\left\{\sqrt{Z_{Ek}^{II}}\right\}\left(V_{E}^{II} + R_{E}^{II}\right)$$

$$J_{HH}^{T}\,\text{Diag}\left\{\sqrt{Y_{Hq}^{I}}\right\}\left(V_{H}^{I} - R_{H}^{I}\right)$$

$$+ J_{EH}^{T}\,\text{Diag}\left\{\sqrt{Y_{Ep}^{I}}\right\}\left(V_{E}^{I} - R_{E}^{I}\right) = \text{Diag}\left\{\sqrt{Y_{Hl}^{II}}\right\}\left(V_{H}^{II} - R_{H}^{II}\right)$$

$$J_{EE}^{T}\,\text{Diag}\left\{\sqrt{Y_{Ep}^{I}}\right\}\left(V_{E}^{I} - R_{E}^{I}\right) = \text{Diag}\left\{\sqrt{Y_{Ek}^{II}}\right\}\left(V_{E}^{II} - R_{E}^{II}\right). \tag{A7}$$

In (A7), $\text{Diag}(f_n)$, denotes a diagonal matrix with elements f_n; T means transposed; and (J) are coupling matrices given by

$$\left(J_{HH}\right)_{ql} = \int_{F^{II}}\left(\text{grad}\,T_{Hq}^{I} \times \vec{e}_z\right)\left(\text{grad}\,T_{Hl}^{II} \times \vec{e}_z\right)dF$$

$$\left(J_{EH}\right)_{pl} = \int_{F^{II}}\left(-\text{grad}\,T_{Ep}^{I}\right)\left(\text{grad}\,T_{Hl}^{II} \times \vec{e}_z\right)dF$$

$$\left(J_{EE}\right)_{pk} = \int_{F^{II}}\text{grad}\,T_{Ep}^{I}\,\text{grad}\,T_{Ek}^{II}\,dF$$

$$\left(J_{HE}\right)_{qk} = \int_{F^{II}}\left(\text{grad}\,T_{Hq}^{I} \times \vec{e}_z\right)\text{grad}\,T_{Ek}^{II}\,dF \equiv 0. \tag{A8}$$

Rearranging forward and backward waves in (A7) yields (5) with the modal scattering matrix (S_S), where the submatrices are given by

$$S_{S11} = -W(U - MM^T)$$

$$S_{S12} = 2WM$$

$$S_{S21} = M^T\{U + W(U - MM^T)\}$$

$$S_{S22} = U - 2M^TWM \tag{A9}$$

with $U = $ unity matrix and

$$W = (U + MM^T)^{-1} \tag{A10}$$

It should be noted that only two complex matrix inversions have to be carried out ((A10) and (A12)) for calculating the modal scattering matrix of the ridge or finned waveguide of finite length.

REFERENCES

[1] S. B. Cohn, "Optimum design of stepped transmission-line transformers," *IRE Trans. Microwave Theory Tech.*, vol. MTT-3, pp. 16–21, Apr. 1955.

[2] S. Hopfer, "The design of ridged waveguide," *IRE Trans. Microwave Theory Tech.*, vol. MTT-3, pp. 20–29, Oct. 1955.

[3] E. S. Hensperger, "Broad-band stepped transformers from rectangular to double-ridged waveguide," *IRE Trans. Microwave Theory Tech.*, vol. MTT–6, pp. 311–314, July 1955.

[4] J. P. Montgomery, "On the complete eigenvalue solution of ridged waveguide," *IEEE Trans. Microwave Theory Tech.*, vol. MTT-19, pp. 547–555, June 1971.

[5] W. J. R. Hoefer and M. N. Burton, "Closed-form expressions for the parameters of finned and ridged waveguides," *IEEE Trans. Microwave Theory Tech.*, vol. MTT-30, pp. 2190–2194, Dec. 1982.

[6] Y. Utsumi, "Variational analysis of ridged waveguide modes," *IEEE Trans. Microwave Theory Tech.*, vol. MTT-33, pp. 111–120, Feb. 1985.

[7] Y. Konishi and K. Uenakada, "The design of a bandpass filter with inductive strip—Planar circuit mounted in waveguide," *IEEE Trans. Microwave Theory Tech.*, vol. MTT-22, pp. 869–873, Oct. 1974.

[8] Y. Konishi, K. Uenakada, N. Yazawa, N. Hoshino, and T. Takahashi, "Simplified 12-GHz low-noise converter with mounted planar circuit in waveguide," *IEEE Trans. Microwave Theory Tech.*, vol. MTT-22, pp. 451–454, Apr. 1974.

[9] Y. Konishi and H. Matsumura, "Short end effect of ridge guide with planar circuit mounted in a waveguide," *IEEE Trans. Microwave Theory Tech.*, vol. MTT-27, pp. 168–170, Feb. 1979.

[10] D. Mirshekar-Syahkal and J. B. Davies, "Accurate analysis of tapered planar transmission lines for microwave integrated circuits," *IEEE Trans. Microwave Theory Tech.*, vol. MTT-29, pp. 123–128, Feb. 1981.

[11] L.-P. Schmidt and H. Meinel, "Broadband millimeter-wave PIN-diode attenuator with double-ridged waveguide flanges," *Electron. Lett.*, vol. 18, no. 19, pp. 839–840, Sept. 1982.

[12] P. J. Meier, "Integrated finline: The second decade," *Microwave J.*, vol. 28, no. 11, pp. 31–54, Nov. 1985; also no. 12, pp. 30–48, Dec. 1985.

[13] R. Sorrentino and T. Itoh, "Transverse resonance analysis of finline discontinuities," in *IEEE MTT-S Int. Symp. Dig.*, 1984, pp. 414–416.

[14] C. J. Verver and W. J. R. Hoefer, "Quarter wave transformers for matching transitions between waveguides and finlines," in *IEEE MTT-S Int. Symp. Dig.*, 1984, pp. 417–419.

[15] P. Pramanick and P. Bhartia, "Analysis and synthesis of tapered fin-lines," in *IEEE MTT-S Int. Symp. Dig.*, 1984, pp. 336–338.

$$M = \begin{bmatrix} \text{Diag}\left\{\sqrt{Y_{Hq}^{I}}\right\}J_{HH}\,\text{Diag}\left\{\sqrt{Z_{Hl}^{II}}\right\} & 0 \\ \text{Diag}\left\{\sqrt{Y_{Ep}^{I}}\right\}J_{EH}\,\text{Diag}\left\{\sqrt{Z_{Hl}^{II}}\right\} & \text{Diag}\left\{\sqrt{Y_{Ep}^{I}}\right\}J_{EE}\,\text{Diag}\left\{\sqrt{Z_{Ek}^{II}}\right\} \end{bmatrix}. \tag{A11}$$

C. Submatrices in (6)

$$S_{R11} = S_{R22} = S_{S11} + S_{S12}D(U - S_{S22}DS_{S22}D)^{-1}S_{S22}DS_{S21}$$

$$S_{R21} = S_{R12} = S_{S12}D(U - S_{S22}DS_{S22}D)^{-1}S_{S21} \tag{A12}$$

where D is a diagonal matrix containing

$$D = \begin{bmatrix} \text{Diag}\left\{\exp\left(-jk_{zHl}^{II}l\right)\right\} & 0 \\ 0 & \text{Diag}\left\{\exp\left(-jk_{zEk}l\right)\right\} \end{bmatrix}. \tag{A13}$$

[16] R. Sorrentino and T. Itoh, "Transverse resonance analysis of finline discontinuities," *IEEE Trans. Microwave Theory Tech.*, vol. MTT-32, pp. 1633–1638, Dec. 1984.

[17] C. Schieblich, J. K. Piotrowski, and J. H. Hinken, "Synthesis of optimum finline tapers using dispersion formulas for arbitrary slot widths and locations," *IEEE Trans. Microwave Theory Tech.*, vol. MTT-32, pp. 1638–1645, Dec. 1984.

[18] C. J. Verver and W. J. R. Hoefer, "Quarter-wave matching of waveguide-to-finline transitions," *IEEE Trans. Microwave Theory Tech.*, vol. MTT-32, pp. 1645–1648, Dec. 1984.

[19] A. Beyer, "Analysis of the transmission characteristics of inhomogeneous grounded finlines," *IEEE Trans. Microwave Theory Tech.*, vol. MTT-33, pp. 145–148, Feb. 1985.

[20] M. Helard, J. Citerne, O. Picon, and V. F. Hanna, "Theoretical and experimental investigation of finline discontinuities," *IEEE Trans. Microwave Theory Tech.*, vol. MTT-33, pp. 994–1003, Oct. 1985.

[21] K. J. Webb and R. Mittra, "Solution of the finline step-discontinuity problem using the generalized variational technique," *IEEE Trans. Microwave Theory Tech.*, vol. MTT-33, pp. 1004–1010, 1985.

[22] R. Vahldieck, J. Bornemann, F. Arndt, and D. Grauerholz, "Optimized waveguide E-plane metal-insert filters for millimeter-wave applications," *IEEE Trans. Microwave Theory Tech.*, vol. MTT-31, pp. 65–69, Jan. 1983.

[23] J. Bornemann, R. Vahldieck, F. Arndt, and D. Grauerholz, "Optimized low-insertion-loss millimetre-wave fin-line and metal insert filters," *Radio Electron. Eng.*, vol. 52, pp. 513–521, Nov./Dec. 1982.

[24] F. Arndt, J. Bornemann, R. Vahldieck, and D. Grauerholz, "E-plane integrated circuit filters with improved stopband attenuation," *IEEE Trans. Microwave Theory Tech.*, vol. MTT-32, pp. 1391–1394, Oct. 1984.

[25] J. R. E. Collin, *Field Theory of Guided Waves*. New York: McGraw-Hill, 1960, ch. 1, ch. 3.4, ch. 5.2.

[26] R. F. Harrington, *Time Harmonic Fields*. New York: McGraw-Hill, 1961, pp. 171–177, 389–425.

[27] H. Patzelt and F. Arndt, "Double-planar steps in rectangular waveguides and their application for transformers, irises, and filters," *IEEE Trans. Microwave Theory Tech.*, vol. MTT-30, pp. 771–776, 1982.

[28] J. Bornemann, "Rigorous field theory analysis of quasiplanar waveguides," *Proc. Inst. Elec. Eng.*, vol. 132, Pt. H, pp. 1–6, Feb. 1985.

[29] R. Vahldieck and J. Bornemann, "A modified mode-matching technique and its application to a class of quasi-planar transmission lines," *IEEE Trans. Microwave Theory Tech.*, vol. MTT-33, pp. 916–926, Oct. 1985.

[30] J. Bornemann and F. Arndt, "Calculating the characteristic impedance of finlines by transverse resonance method," *IEEE Trans. Microwave Theory Tech.*, vol. MTT-34, pp. 85–92, Jan. 1986.

[31] H. D. Knetsch, "Beitrag zur Theorie sprunghafter Querschnittsveränderungen von Hohlleitern," *Arch. Elek. Übertragung*, vol. 22, pp. 591–600, Dec. 1968.

[32] H. Schmiedel, "Anwendung der Evolutionsoptimierung bei Mikrowellenschaltungen," *Frequenz*, vol. 35, pp. 306–310, Nov. 1981.

[33] T. E. Rozzi and W. F. G. Mecklenbräuker, "Wide-band network modeling of interacting inductive irises and steps," *IEEE Trans. Microwave Theory Tech.*, vol. MTT-23, pp. 235–245, Feb. 1975.

[34] M. S. Navarro, T. E. Rozzi, and Y. T. Lo, "Propagation in a rectangular waveguide periodically loaded with resonant irises," *IEEE Trans. Microwave Theory Tech.*, vol. MTT-28, pp. 857–865, Aug. 1980.

[35] F. Arndt, B. Koch, H.-J. Orlok, and N. Schröder, "Field theory design of rectangular waveguide broad-wall metal-insert slot couplers for millimeter-wave applications," *IEEE Trans. Microwave Theory Tech.*, vol. MTT-33, pp. 95–104, Feb. 1985.

✱

Jens Bornemann was born in Hamburg, West Germany, on May 26, 1952. He received the Dipl. Ing. and the Dr. Ing. degrees, both in electrical engineering, from the University of Bremen, Bremen, West Germany, in 1980 and 1984, respectively.

From 1980 to 1983, he was a Research Assistant at the Microwave Department of the University of Bremen, where he worked on quasi-planar waveguide configurations and computer-aided E-plane filter design. After a two-year period as a consulting engineer, he joined the University of Bremen again, in 1985. His current research activities include millimeter-wave integrated circuit components and problems of electromagnetic field theory, especially those requiring numerical methods of solution.

Dr. Bornemann was one of the recipients of the A. F. Bulgin Premium of the Institution of Electronic and Radio Engineers (1983).

✱

Fritz Arndt (SM'83) was born in Konstanz, Germany, on April 30, 1938. He received the Dipl. Ing., Dr. Ing., and Habilitation degrees from the Technical University of Darmstadt, Germany, in 1963, 1968, and 1972, respectively.

From 1963 to 1973, he worked on directional couplers and microstrip techniques at the Technical University of Darmstadt. Since 1972, he has been a Professor and Head of the Microwave Department of the University of Bremen, Germany. His research activities are in the area of the solution of field problems of waveguide, finline, and optical waveguide structures, of antenna design, and of scattering structures.

Dr. Arndt is member of the VDE and NTG (Germany). He received the NTG award in 1970, the A. F. Bulgin Award (together with three coauthors) from the Institution of Radio and Electronic Engineers in 1983, and the best paper award of the antenna conference JINA 1986 (France).